

Evidence for a Field-induced Quantum Spin Liquid in α -RuCl₃

S.-H. Baek,^{1,*} S.-H. Do,² K.-Y. Choi,^{2,†} Y. S. Kwon,³ A.U.B. Wolter,¹ S. Nishimoto,^{1,4} Jeroen van den Brink,^{1,4} and B. Büchner^{1,4}

¹*IFW Dresden, Helmholtzstr. 20, 01069 Dresden, Germany*

²*Department of Physics, Chung-Ang University, Seoul 156-756, Republic of Korea*

³*Department of Emerging Materials Science, DGIST, Daegu 711-873, Republic of Korea*

⁴*Department of Physics, Technische Universität Dresden, 01062 Dresden, Germany*

(Dated: July 20, 2017)

We report a ³⁵Cl nuclear magnetic resonance study in the honeycomb lattice α -RuCl₃, a material that has been suggested to potentially realize a Kitaev quantum spin liquid (QSL) ground state. Our results provide direct evidence that α -RuCl₃ exhibits a magnetic-field-induced QSL. For fields larger than ~ 10 T, a spin gap opens up while resonance lines remain sharp, evidencing that spins are quantum disordered and locally fluctuating. The spin gap increases linearly with an increasing magnetic field, reaching ~ 50 K at 15 T, and is nearly isotropic with respect to the field direction. The unusual rapid increase of the spin gap with increasing field and its isotropic nature are incompatible with conventional magnetic ordering and, in particular, exclude that the ground state is a fully polarized ferromagnet. The presence of such a field-induced gapped QSL phase has indeed been predicted in the Kitaev model.

When the interactions between magnetic spins are strongly frustrated, quantum fluctuations can cause spins to remain disordered even at very low temperatures [1]. The quantum spin liquid (QSL) state that ensues is conceptually very interesting – for instance, new fractionalized excitations appear that are very different from the ordinary spin-wave excitations in ordered magnets [2–5]. A QSL appears in the so-called Kitaev honeycomb model – a prototypical and mathematically well-understood model of strongly frustrated interacting spins [6, 7]. In an external magnetic field the topological QSL state acquires a gap that, in the generic case grows linearly with field strength [8].

This observation has motivated the search for the experimental realization of the Kitaev honeycomb model and its topological QSL phases. The quest was centered, until recently, mainly on honeycomb iridate materials [9, 10] of the type $A_2\text{IrO}_3$ ($A = \text{Na}$ or Li). However, in these iridates long-range magnetic order develops at low temperatures for all known different crystallographic phases [11–15]. Their QSL regime is most likely preempted by the presence of significant residual Heisenberg-type interactions, by longer-range interactions between the spins or by crystallographically distinct Ir-Ir bonds, if not by a combination of these factors [16–19]. More promising in this respect is ruthenium trichloride α -RuCl₃ in its honeycomb crystal phase, as numerous experimental and theoretical studies pointed the significance of the anisotropic Kitaev exchange in the material [20–27]. Neutron scattering studies have shown that the magnetic interactions in this material are closer to the Kitaev limit [28], although at low temperatures also this quasi-2D material exhibits long-range magnetic order.

In this Letter, we show by means of nuclear magnetic resonance (NMR) that in α -RuCl₃ large magnetic fields

larger than ~ 10 T melt the magnetic order, and a spin-gap opens that scales linearly with the magnetic field, implying that the detrimental effects of residual magnetic interactions between the Ru moments can be overcome by an external magnetic field that stabilizes a QSL state.

³⁵Cl (nuclear spin $I = 3/2$) NMR was carried out in a α -RuCl₃ single crystal as a function of external field (H) and temperature (T). (See Supplemental Material for the crystal growth and characterization.) The sample was reoriented using a goniometer for the accurate alignment along \mathbf{H} . The ³⁵Cl NMR spectra were acquired by a standard spin-echo technique with a typical $\pi/2$ pulse length 2–3 μs . The nuclear spin-lattice relaxation rate T_1^{-1} was obtained by fitting the recovery of the nuclear magnetization $M(t)$ after a saturating pulse to the following fitting function: $1 - M(t)/M(\infty) = A[0.9e^{-(6t/T_1)^\beta} + 0.1e^{-(t/T_1)^\beta}]$, where A is a fitting parameter and β is the stretching exponent.

Experimentally, in α -RuCl₃, a very peculiar strongly anisotropic magnetism has been reported [24–26] based on measurements of the uniform magnetic susceptibility χ and the specific heat C_p/T . From the data it is clear that the antiferromagnetic (AFM) state observed at low T is hardly affected by external fields along the c direction whereas the signatures of the long-range magnetic order seen in C_p/T and $\chi(T)$ disappear for moderate fields of about 8 T applied along the ab plane. This pronounced anisotropy of the magnetism is also found in our crystals (see Fig. 1a and b). Note that whereas earlier studies [25, 26, 29] reported either two magnetic transitions at $T_{N1} \sim 8$ K and $T_{N2} \sim 14$ K or a single transition at $T_N \sim 13$ K, our measurements show, essentially, a single transition occurring at a considerably lower temperature, $T_{N1} \sim 6.2$ K. This evidences that our sample is of high quality with a (nearly) uniform stacking pattern [28, 30].

We now turn to the ³⁵Cl NMR measurements on α -

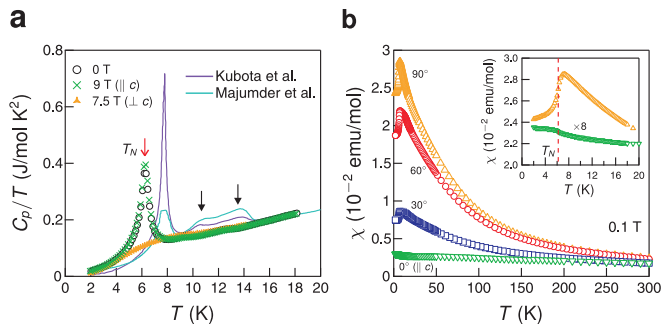


FIG. 1. **a**, Low- T specific heat C_p/T at zero and chosen magnetic fields. The data at zero field taken from Refs. [26] and [25] are compared. **b**, Temperature dependence of the uniform magnetic susceptibility χ at $H = 0.1$ T obtained for the four different field orientations with respect to the c axis. The inset enlarges the low- T region.

RuCl₃. Since the ³⁵Cl nuclei possess a large quadrupole moment, the NMR spectra are strongly affected by the electric field gradient (EFG). In α -RuCl₃, the principal axis of the largest eigenvalue of the EFG tensor V_{zz} at ³⁵Cl is expected to point along the shared edges of the RuCl₆ octahedra which are tilted $\sim 35^\circ$ away from the c axis as illustrated in Fig. 2a.

As a result, there exist three inequivalent ³⁵Cl sites, yielding a very complex and broad ³⁵Cl spectrum in a magnetic field, as shown in Fig. 2b, which would make further NMR studies extremely difficult. However, taking advantage of the fact that the influence of the quadrupole interaction is very sensitive to the angle between the direction of V_{zz} ($\equiv \hat{V}_{zz}$) and H , it is possible to separate one ³⁵Cl spectrum from other two spectra by applying H along one of the three local directions of V_{zz} at ³⁵Cl. Moreover, when $H \parallel \hat{V}_{zz}$, the quadrupole line broadening should be significantly reduced, allowing further narrowing of the line.

Indeed, by rotating the sample in the ac plane, we achieved a very narrow single ³⁵Cl line with the linewidth of 10 kHz at $\theta \sim 30^\circ$ (see Fig. 2b). When the sample is reversely rotated by 90° (i.e., $H \perp \hat{V}_{zz}$), we also detected a narrow ³⁵Cl line. These observations confirm that V_{zz} is directed $\sim 30^\circ$ from the c axis. Therefore, it is very convenient to define $\hat{V}_{zz} \equiv c'$, and we, in the following, will present our NMR results with respect to the c' axis.

The T dependence of the ³⁵Cl NMR spectrum at 15 T is presented in Fig. 2c. Clearly, there is no signature of long-range magnetic order, which would cause a large broadening or splitting of the ³⁵Cl line. Another feature is the appearance of a new NMR peak that replaces the original one below ~ 75 K. This is due to a first order structural phase transition [24, 26]; details are provided in the Supplemental Material.

Figure 2d presents the T -dependence of the resonance frequency ν in terms of the NMR shift $\mathcal{K} = (\nu - \nu_0)/\nu_0$ where ν_0 is the unshifted Larmor frequency. \mathcal{K} is com-

posed, mainly, of the three terms: $\mathcal{K} = A_{\text{hf}}\chi_{\text{spin}} + \mathcal{K}_{\text{chem}} + \mathcal{K}_{\text{quad}}$ where A_{hf} is the hyperfine (hf) coupling constant, χ_{spin} the local spin susceptibility, $\mathcal{K}_{\text{chem}}$ the T independent chemical shift, and $\mathcal{K}_{\text{quad}}$ the second order quadrupole shift. Since $\mathcal{K}_{\text{quad}}$ which is determined by the charge distribution around the ³⁵Cl nucleus weakly changes with T [31], the strong upturn of \mathcal{K} observed at low T has to be attributed to χ_{spin} which is consistent with the macroscopic susceptibility (see Fig. 1c).

Figure 2e shows the T dependence of T_1^{-1} at $H = 15$ T. At high $T > T^* \sim 160$ K, T_1^{-1} follows roughly the behavior expected for simple paramagnets; T_1^{-1} is nearly independent of T . The different absolute values of T_1^{-1} for the two orientations of H are ascribed to the anisotropic hf couplings (see Fig. 2d).

As T is lowered below T^* , T_1^{-1} increases for $H \parallel c'$ but it decreases for $H \perp c'$. Since the spin-lattice relaxation process is induced by the transverse components of spin fluctuations (SFs) with respect to the nuclear quantization axis, it is clear that T_1^{-1} for $H \parallel c'$ experiences stronger in-plane and weaker out-of-plane SFs than for $H \perp c'$. Hence, the increase of the T_1^{-1} anisotropy with lowering T is an indication of the development of strong in-plane SFs below T^* .

At low temperatures, roughly below 50 K, T_1^{-1} starts to decrease. For the study of spin dynamics at low T , it is convenient to consider the quantity $(T_1 T)^{-1}$, which is proportional to the \mathbf{q} -average of the imaginary part of the dynamical susceptibility, $\sum_{\mathbf{q}} A_{\text{hf}}^2(\mathbf{q})\chi''(\mathbf{q}, \omega_0)/\omega_0$, where ω_0 is the Larmor resonance frequency. As shown in Fig. 3a, a broad maximum of $(T_1 T)^{-1}$ occurs near 30 K, being followed by a rapid drop towards low T in an identical manner for both field orientations. The rapid decrease of $(T_1 T)^{-1}$ implies a pronounced depletion of spectral weight in the spin excitation spectrum. The semilog plot of T_1^{-1} against $1/T$ drawn in Fig. 3b unambiguously reveals a spin gap behavior, $T_1^{-1} \propto \exp(-\Delta/T)$, with the gap $\Delta \sim 44$ and 50 K for $H \parallel c'$ and $\perp c'$, respectively.

An explanation of the observed spin gap in terms of static magnetic order can be ruled out. For example, the ³⁵Cl spectra measured at $H = 15$ T do not show any signature of magnetic order down to 4.2 K (see Fig. 2c). Moreover, it is difficult to attribute the extracted large spin gap to some kind of anisotropy gap occurring in the spin wave spectrum in magnetically ordered systems. As displayed in Fig. 3a, the low temperature behavior of $(T_1 T)^{-1}$ is very similar for both field orientations, indicating that spin dynamics is nearly isotropic at least in the range of field orientations ($30^\circ - 60^\circ$ off the ab plane). Therefore, not only the measured large gap size, but also the isotropic gap behavior, contradicts any interpretation in terms of anisotropy gaps. The findings are also incompatible with the gap being due to a saturating ferromagnetic (FM) polarization of spins. The magnetization near 10 T is far less than the saturated value [29], particularly for $H \parallel c'$. For this field orientation, the g

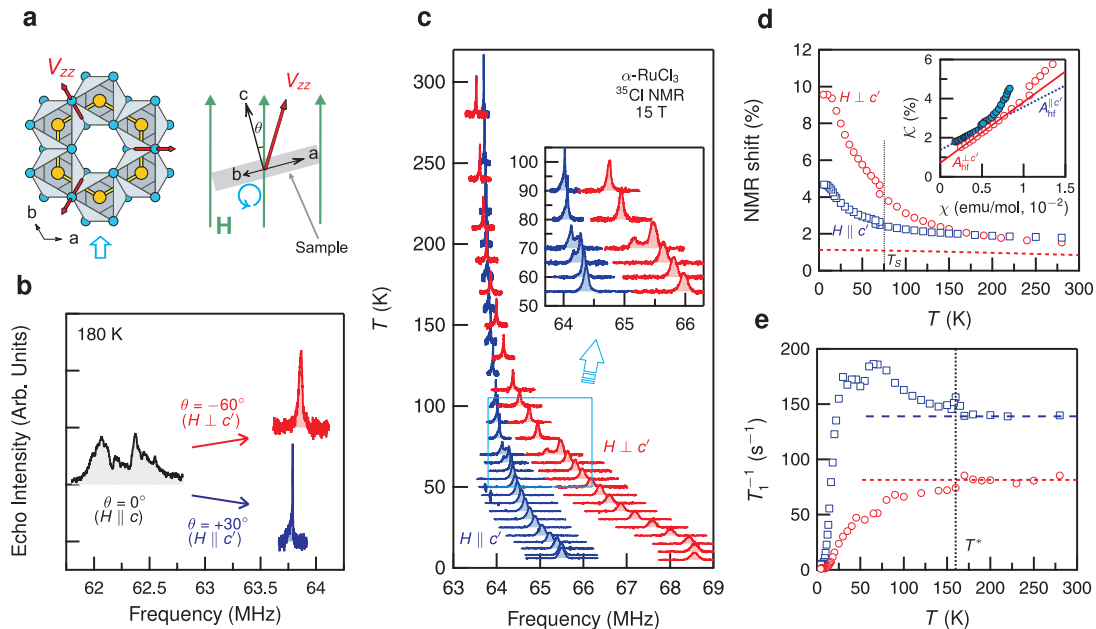


FIG. 2. **a**, The principal axis of the EFG V_{zz} at the ^{35}Cl nuclei is along the shared edges of the RuCl_6 octahedra, resulting in three inequivalent ^{35}Cl sites in field. The sample is mounted on the goniometer so that one of the three axes of V_{zz} 's lies in the rotating plane. **b**, When $H \parallel c$ ($\theta = 0$), the ^{35}Cl spectrum is extremely complex and broad. As H is either parallel or perpendicular to the direction of V_{zz} , very narrow ^{35}Cl NMR lines were obtained. **c**, ^{35}Cl NMR spectrum measured at $H = 15$ T as a function of T with cooling for two different field orientations. The first order character of the structural transition is evidenced by the gradual transfer of the ^{35}Cl spectral weight below $T_S \sim 75$ K, as clearly shown in the inset. **d**, NMR shift \mathcal{K} as a function of T . The strong anisotropy of \mathcal{K} increases rapidly with decreasing T , approaching a saturated value below ~ 10 K. The dotted line is the estimated T dependence of $\mathcal{K}_{\text{quad}}$ (see SM). The inset shows the \mathcal{K} vs χ plot, which yields the hyperfine coupling constants, $A_{\text{hf}}^{\perp c'} = 17.4$ kG/ μ_B and $A_{\text{hf}}^{\parallel c'} = 12.3$ kG/ μ_B . **e**, Spin-lattice relaxation rate T_1^{-1} vs. T . Whereas T_1^{-1} is nearly T -independent above $T^* = 160$ K, it increases (decreases) for $H \parallel c'$ ($H \perp c'$) below T^* , implying the development of in-plane spin correlations.

factor is also very small, estimated to be $\sim 1\mu_B/\text{Ru}^{3+}$ [26], which is an order of magnitude smaller than the required value 13.4 for the slope between the gap and the field shown in Fig. 4b. This clear-cut conclusion from the bare experimental findings is further supported by a detailed theoretical analysis (see Supplemental Material).

In order to study the H dependence of Δ , we measured T_1^{-1} as a function of $H \parallel c'$ at low T . The results are shown in Fig. 3c and 3d. A spin gap is only seen for $H > 10$ T and Δ increases with increasing H . At $H = 10$ T our data show a Curie-like upturn of the SFs, i.e., $(T_1 T)^{-1}$ diverges for low T . Upon further lowering H below 10 T, a sharp peak in $(T_1 T)^{-1}$ signals static magnetic order below T_N which decreases with increasing H . Below T_N , the ^{35}Cl spectrum progressively spreads out with decreasing T , indicating the incommensurate character of AFM order [25]; the spectra in the paramagnetic and magnetically ordered states are compared in the Supplemental Material. Thus, our data for $(T_1 T)^{-1}$ clearly show a qualitative change of the behavior as a function of H : the peak due to static order occurring at low field is replaced by a spin gap behavior at $H \geq 10$ T. At the border the spin dynamics suggests quantum

criticality, i.e. a divergence of $(T_1 T)^{-1}$ for $T = 0$. To back our NMR findings, we measured C_p/T for $H \parallel c'$ (Fig. 4a). The anomaly associated with AFM order is rapidly suppressed toward 10 T, which perfectly agrees with the T_1^{-1} results. Further, we confirmed that at 14 T C_p/T is significantly suppressed at low T , evidencing the opening of a spin gap at $H > 10$ T [32].

The data thus indicate a field-induced crossover from a magnetically ordered state at low fields to a disordered state showing gapped spin excitations in large fields. Moreover, as evident from Fig. 3d, the field dependence of $T_1^{-1}(T)$ reveals that Δ increases linearly with H above 10 T [33]. Extrapolating the curve to lower fields yields a threshold value of $H_c \sim 10$ T, i.e. the same field where the T -dependence of the T_1^{-1} changes its qualitative behavior from an upturn to a downturn at low T . Fig. 3d also shows a low T flattening out of T_1^{-1} indicating the presence of another very low energy scale for spin dynamics. This feature is likely related to inhomogeneous states, for instance, due to magnetic defects. It becoming suppressed with increasing H is consistent with competition between partially defect-induced magnetism and a spin gap that increases with H . Our findings are sum-

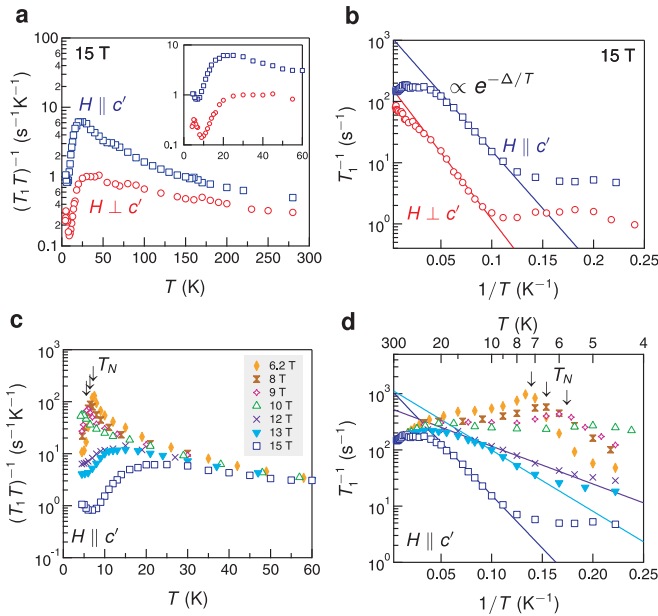


FIG. 3. **a**, $(T_1T)^{-1}$ as a function of T measured at 15 T. At low T , $(T_1T)^{-1}$ for both field directions reaches a maximum at ~ 25 K which is followed by a rapid drop upon further cooling. Inset enlarges the low T region. **b**, Semilog plot of T_1^{-1} vs. $1/T$ unravels a spin gap behavior $T_1^{-1} \propto \exp(-\Delta/T)$. The deviation from the gap behavior takes place below ~ 10 K. **c**, Strong field dependence of $(T_1T)^{-1}$ at low T as a function of $H_{\parallel c'}$. Below 9 T, AFM ordered phase was clearly detected by sharp peaks of $(T_1T)^{-1}$. **d**, The spin gap Δ is rapidly filled up with decreasing $H_{\parallel c'}$, vanishing completely at 10 T.

marized in the H - T phase diagram, see Fig. 4b [34].

Previously it was established on theoretical and experimental grounds that the magnetic interactions between the quantum spins in α - RuCl_3 are well described by the Kitaev model, however in the presence of residual interactions which ultimately preempt the QSL state in a zero magnetic field [20–26, 28, 35]. In the pure Kitaev model at zero field, the ground state is an Abelian QSL that is gapless [6], and the present observations suggest that the absence of a gap leaves this Abelian QSL very susceptible to the perturbing residual interactions that drive the formation of long-range magnetic order. In a finite field, however, a non-Abelian QSL forms in the pure honeycomb Kitaev model, which is protected by a spin gap [6]. The data suggest that when the magnetic field and gap become large enough, it can overcome the energy scale related to the residual magnetic interactions so that a QSL emerges.

This work has been supported by the Deutsche Forschungsgemeinschaft (Germany) via DFG Research Grants BA 4927/1-3 and the collaborative research center SFB 1143. JvdB acknowledges support from the Harvard-MIT CUA.

Note Added.— Recent thermal transport [36] and specific heat [37] measurements verified the field-induced

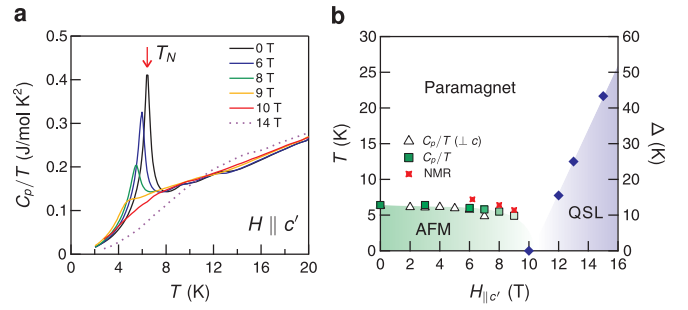


FIG. 4. **a**, The dependence of C_p/T at $H \parallel c'$ oriented along c' . With increasing H , AFM order is suppressed and completely disappears at 10 T - at 14 T a gap appears to be present. **b**, The T - H phase diagram obtained by NMR and specific heat measurements. T_N obtained by specific heat for $H \perp c$ is compared. In the QSL region the field dependence of the spin-gap Δ is shown (right axis).

gapped phase in α - RuCl_3 , in great support of our work. Interestingly, we find some detailed quantitative differences, e.g., for the critical field, the slope of the gap vs field, and the anisotropy of the gap. These are ascribed to the fact that the temperature and field regime considered in these studies are quite lower than ours. This suggests that the spin gap behavior critically changes when approaching the quantum critical point—which is an interesting subject for future study.

* sbaek.fu@gmail.com

† kchoi@cau.ac.kr

- [1] L. Balents, *Nature* **464**, 199 (2010).
- [2] Y. Shimizu, K. Miyagawa, K. Kanoda, M. Maesato, and G. Saito, *Phys. Rev. Lett.* **91**, 107001 (2003).
- [3] M. Yamashita, N. Nakata, Y. Senshu, M. Nagata, H. M. Yamamoto, R. Kato, T. Shibauchi, and Y. Matsuda, *Science* **328**, 1246 (2010).
- [4] T.-H. Han, J. S. Helton, S. Chu, D. G. Nocera, J. A. Rodriguez-Rivera, C. Broholm, and Y. S. Lee, *Nature* **492**, 406 (2012).
- [5] M. Fu, T. Imai, T.-H. Han, and Y. S. Lee, *Science* **350**, 655 (2015).
- [6] A. Kitaev, *Annals of Physics* **321**, 2 (2006).
- [7] J. K. Pachos, *Introduction to Topological Quantum Computation* (Cambridge University Press, Cambridge, UK, 2012).
- [8] X.-Y. Song, Y.-Z. You, and L. Balents, *Phys. Rev. Lett.* **117**, 037209 (2016).
- [9] G. Jackeli and G. Khaliullin, *Phys. Rev. Lett.* **102**, 017205 (2009).
- [10] J. Chaloupka, G. Jackeli, and G. Khaliullin, *Phys. Rev. Lett.* **105**, 027204 (2010).
- [11] Y. Singh and P. Gegenwart, *Phys. Rev. B* **82**, 064412 (2010).
- [12] F. Ye, S. Chi, H. Cao, B. C. Chakoumakos, J. A. Fernandez-Baca, R. Custelcean, T. F. Qi, O. B. Korneta, and G. Cao, *Phys. Rev. B* **85**, 180403 (2012).

- [13] S. K. Choi, R. Coldea, A. N. Kolmogorov, T. Lancaster, I. I. Mazin, S. J. Blundell, P. G. Radaelli, Y. Singh, P. Gegenwart, K. R. Choi, S.-W. Cheong, P. J. Baker, C. Stock, and J. Taylor, *Phys. Rev. Lett.* **108**, 127204 (2012).
- [14] T. Takayama, A. Kato, R. Dinnebier, J. Nuss, H. Kono, L. Veiga, G. Fabbris, D. Haskel, and H. Takagi, *Phys. Rev. Lett.* **114**, 077202 (2015).
- [15] K. A. Modic, T. E. Smidt, I. Kimchi, N. P. Breznay, A. Biffin, S. Choi, R. D. Johnson, R. Coldea, P. Watkins-Curry, G. T. McCandless, J. Y. Chan, F. Gandara, Z. Islam, A. Vishwanath, A. Shekhter, R. D. McDonald, and J. G. Analytis, *Nature Communications* **5**, 4203 (2014).
- [16] I. Kimchi and Y.-Z. You, *Phys. Rev. B* **84**, 180407 (2011).
- [17] J. G. Rau, E. K.-H. Lee, and H.-Y. Kee, *Phys. Rev. Lett.* **112**, 077204 (2014).
- [18] V. M. Katukuri, S. Nishimoto, V. Yushankhai, A. Stoyanova, H. Kandpal, S. Choi, R. Coldea, I. Rousochatzakis, L. Hozoi, and J. van den Brink, *New Journal of Physics* **16**, 013056 (2014).
- [19] S. Nishimoto, V. M. Katukuri, V. Yushankhai, H. Stoll, U. K. Rößler, L. Hozoi, I. Rousochatzakis, and J. van den Brink, *Nature Communications* **7**, 10273 (2016).
- [20] K. W. Plumb, J. P. Clancy, L. J. Sandilands, V. V. Shankar, Y. F. Hu, K. S. Burch, H.-Y. Kee, and Y.-J. Kim, *Phys. Rev. B* **90**, 041112 (2014).
- [21] I. Rousochatzakis, J. Reuther, R. Thomale, S. Rachel, and N. B. Perkins, *Phys. Rev. X* **5**, 041035 (2015).
- [22] H.-S. Kim, V. S. Shankar V., A. Catuneanu, and H.-Y. Kee, *Phys. Rev. B* **91**, 241110 (2015).
- [23] L. J. Sandilands, Y. Tian, A. A. Reijnders, H.-S. Kim, K. W. Plumb, Y.-J. Kim, H.-Y. Kee, and K. S. Burch, *Phys. Rev. B* **93**, 075144 (2016).
- [24] J. A. Sears, M. Songvilay, K. W. Plumb, J. P. Clancy, Y. Qiu, Y. Zhao, D. Parshall, and Y.-J. Kim, *Phys. Rev. B* **91**, 144420 (2015).
- [25] M. Majumder, M. Schmidt, H. Rosner, A. A. Tsirlin, H. Yasuoka, and M. Baenitz, *Phys. Rev. B* **91**, 180401 (2015).
- [26] Y. Kubota, H. Tanaka, T. Ono, Y. Narumi, and K. Kindo, *Phys. Rev. B* **91**, 094422 (2015).
- [27] J. Nasu, J. Knolle, D. L. Kovrizhin, Y. Motome, and R. Moessner, *Nature Physics* **12**, 912 (2016).
- [28] A. Banerjee, C. A. Bridges, J.-Q. Yan, A. A. Aczel, L. Li, M. B. Stone, G. E. Granroth, M. D. Lumsden, Y. Yiu, J. Knolle, S. Bhattacharjee, D. L. Kovrizhin, R. Moessner, D. A. Tennant, D. G. Mandrus, and S. E. Nagler, *Nature Mater.* **15**, 733 (2016).
- [29] R. D. Johnson, S. C. Williams, A. A. Haghighirad, J. Singleton, V. Zapf, P. Manuel, I. I. Mazin, Y. Li, H. O. Jeschke, R. Valentí, and R. Coldea, *Phys. Rev. B* **92**, 235119 (2015).
- [30] H. B. Cao, A. Banerjee, J.-Q. Yan, C. A. Bridges, M. D. Lumsden, D. G. Mandrus, D. A. Tennant, B. C. Chakoumakos, and S. E. Nagler, *Phys. Rev. B* **93**, 134423 (2016).
- [31] E. N. Kaufmann and R. J. Vianden, *Rev. Mod. Phys.* **51**, 161 (1979).
- [32] Our analysis of the data at low T yields $\Delta \sim 20$ K at 13.9 T (see SM for details) in rough agreement with the NMR findings.
- [33] It is interesting to note that for the pure Kitaev model a magnetic field generates in lowest-order perturbation theory an excitation gap proportional to the field cubed [6]. In α - RuCl_3 certainly magnetic interactions beyond the pure Kitaev exchange are of relevance [22, 24, 28, 38]—how the perturbation results for the pure model are affected by the significant residual interactions in the presence of a magnetic field is, at the moment, an open theoretical question.
- [34] Note that the suppression of AFM order for $H \parallel c'$ occurs at ~ 10 T, which is only slightly higher than ~ 9 T observed for $H \parallel ab$. This observation is striking because for $H \parallel c'$ the field strength projected to the honeycomb plane is only half of the applied one. This suggests that the AFM order is robust only when H is nearly parallel to the normal direction of the plane.
- [35] L. J. Sandilands, Y. Tian, K. W. Plumb, Y.-J. Kim, and K. S. Burch, *Phys. Rev. Lett.* **114**, 147201 (2015).
- [36] R. Hentrich, A. U. B. Wolter, X. Zotos, W. Brenig, D. Nowak, A. Isaeva, T. Doert, A. Banerjee, P. Lampen-Kelley, D. G. Mandrus, S. E. Nagler, J. Sears, Y.-J. Kim, B. Büchner, and C. Hess, arXiv:1703.08623 (unpublished).
- [37] J. A. Sears, Y. Zhao, Z. Xu, J. W. Lynn, and Y.-J. Kim, *Phys. Rev. B* **95**, 180411 (2017).
- [38] R. Yadav, N. A. Bogdanov, V. M. Katukuri, S. Nishimoto, J. van den Brink, and L. Hozoi, *Sci. Rep.* **6**, 37925 (2016).